Density Functional Theory Simulations and Experimental Measurements of a-HfO_2/a-Si_3N_4/SiGe, a-HfO_2/$SiO_{0.8}N_{0.8}$/SiGe and a-HfO_2/a-SiO/SiGe interfaces.

E. Chagarov[1], K. Sardashti[1], M. Edmonds[1], M. Clemons[1], A. Kummel[1]
[1] University of California, San Diego, La Jolla, CA, 92093 USA, email: echagarov@ucsd.edu

***Abstract*—**A comprehensive set of density functional theory (DFT) molecular dynamics (MD) simulations is presented for interfaces between a-HfO_2 high-K oxide and $Si_{0.5}Ge_{0.5}$(001) with several amorphous stoichiometric and sub-stoichiometric SiOxNy interlayers (a-$SiO_{0.8}N_{0.8}$, a-$SiO_{0.4}N_{0.4}$, a-Si_3N_2, a-Si_3N_4 and a-SiO) to determine their electrical passivation properties. In general the sub-stoichiometric interlayers had superior electrical properties because they minimized Ge-O and Ge-N bond formation and had low internal bond strain. The stack with oxygen deficient a-SiO interlayer demonstrated superior electric properties because it avoided all dangling bond formation. Experimental studies confirmed that a sub-stiochiometric SiON layer decreases the defects density of HfO_2(001)/$Si_{0.5}Ge_{0.5}$(001) MOSCAPs.

I. Introduction

To increase both n-channel and p-channel mobility, advance logic devices have transitioned to SiGe-based FinFET structures. Formation of high-k gate oxide/SiGe interfaces is challenging since germanium suboxide (GeO_x<2 containing Ge^{+2}) is known to induce electronic defects and it is nearly impossible to fully oxidize or nitride Ge to Ge^{+4} in the presence of Si since both O and N make stronger bonds to Si than Ge. An alternative approach is to form a monolayer or bilayer of amorphous SiOxNy between the high-k dielectric and the SiGe channel. This can be done by either ALD of silicon monolayers/bilayer or annealing of an SiGeON interface to form a purely SiON layer [1-3]. However, the ideal composition of the SiON layer is unknown. A fully stoichiometric layer has the advantage of the widest possible bandgap but its formation in the presence of excess Ge atoms in the channel is problematic.

II. Density-Functional Theory Simulations.

DFT-MD simulations were employed to form bilayers of a-$SiO_{0.8}N_{0.8}$, a-$SiO_{0.4}N_{0.4}$, a-Si_3N_2, a-Si_3N_4 and a-SiO interlayers on SiGe(001) by random placing O and N atoms on SiGe(001), annealing stacks at 800K, cooling to 0K and relaxing to the ground state configuration below force tolerance level of 0.05 eV/Å. The 3 bottom SiGe layers were fixed in the bulk-like positions and passivated by H atoms to simulate continuous bulk. After interlayer formation, the a-HfO_2 sample was stacked on the relaxed interlayer/SiGe stacks and annealed-cooled-relaxed as described previously. The present DFT-MD simulations employed high-quality amorphous HfO_2 sample generated by separate DFT-MD "melt-and-quench" runs described elsewhere [4-6]. The DFT-MD simulations were performed using the VASP plane-wave simulation package using projector augmented-wave (PAW) pseudopotentials (PP) and Perdew, Burke and Ernzerhof (PBE) exchange-correlation functional [7-14]. The density of states was calculated with HSE06 exchange-correlation hybrid-functional [15-17].

For silicon nitride passivation, a comparison was made between a sub-stoichiometric N-deficient interlayer (a-HfO_2/a-Si_3N_2/SiGe interlayer (see Fig 1a) and a fully-stoichiometric nitride interlayer (a-HfO_2/a-Si_3N_4/SiGe) (see Fig 1b). While the a-HfO_2/a-Si_3N_4/SiGe has multiple Ge-N bonds, the a-HfO_2/a-Si_3N_2/SiGe has no Ge-N bonds since there are sufficient Si atoms in the interface to satisfy all N bonding. However, the sub-stoichiometric a-HfO_2/a-Si_3N_2/SiGe stack has several pinning states (Fig. 2-a). The band-decomposed charge density for VB edge states [-0.7; -0.2] (eV) shows that they originate from a 3-fold under-coordinated Si atom and a 6-fold coordinated Si atom with strained bonding while the CB edge states [-0.2; +0.3] (eV) are induced by 3-fold under-coordinated Si atom and 6-fold coordinated Si atom with strained bonding (Fig 3). For both energy intervals, the pinning states are localized at the a-Si_3N_2/SiGe interface and can be attributed to the significant interface deformation.

The HSE06 DOS curve shown in Fig 2-b for the stoichiometric a-HfO_2/a-Si_3N_4/SiGe stack (red curve) and a-HfO_2/a-Si_3N_2/SiGe (black curve). The DOS for the a-HfO_2/a-Si_3N_4/SiGe stack still has pinning states in the bandgap. The HSE06 band-decomposed charge density of the states near the VB [-0.2; +0.1] and near the CB [+0.1; +0.75] (eV) show they are both induced by the same 3-fold under-coordinated Ge atom (Fig 4). The pinning states are localized at the a-Si_3N_4/SiGe interface and consistent with the interface deformation. In sum, for both purely nitride interfaces, the ridged, strong bonds in the SiNx interlayer induced deformations in the top layer of SiGe which pinned the Fermi level.

For silicon oxynitride passivation, a comparison was made between a sub-stoichiometric O/N-deficient interlayer a-

HfO_2/a-$SiO_{0.4}N_{0.4}$/SiGe (see Fig 5-a) and a fully-stoichiometric SiON interlayer a-HfO_2/a-$SiO_{0.8}N_{0.8}$/SiGe (see Fig 5-b). While the stoichiometric interface had 4 Ge-N and 1 Ge-O bonds, there are no Ge-O or Ge-N bonds in the sub-stoichiometric interface. The HSE06 DOS curves demonstrate that the a-HfO_2/a-$SiO_{0.4}N_{0.4}$/SiGe has an unpinned bandgap with minor band-edge states (Fig. 6-a). The band-decomposed charge density of the VB edge states [0.0; +0.6] (eV) show they originate at a 3-fold under-coordinated Ge (Fig. 7). This Ge atom is located below a-$SiO_{0.8}N_{0.8}$/SiGe interface loosing a bond to an Si atom, which switched its bond to O atom.

The HSE06 DOS curve for the a-HfO_2/a-$SiO_{0.8}N_{0.8}$/SiGe stack (see Fig. 6-b) demonstrates a pinned interface (red curve) with almost zero band-gap in contrast to the a-HfO_2/a-$SiO_{0.4}N_{0.4}$/SiGe stack (black curve). The HSE06 band-decomposed charge density of the VB [-1.0; -0.5] and CB [-0.5; 0.0] (eV) states demonstrates that for a-HfO_2/a-$SiO_{0.8}N_{0.8}$/SiGe the VB states are induced by a 3-fold under-coordinated Ge atom and fully-coordinated Ge with strained bonding while the CB states are induced by the same Ge atom with strained bonding (Fig. 8). Similar to the a-Si_3N_4/SiGe interface, the pinning defects are localized at the a-$SiO_{0.8}N_{0.8}$/SiGe interface and caused by interface deformation.

For silicon oxide passivation, a sub-stoichiometric O-deficient interlayer, the a-HfO_2/a-SiO/SiGe stack was simulated (Fig 9); there is just one Ge-O bond since there are sufficient Si atoms in the interface to satisfy nearly all O bonding. The calculated HSE06 DOS is nearly ideal and demonstrates unpinned bandgap with no Fermi-level shifting (Fig. 9). The high quality of this interface can be explained by almost perfect coordination of interfacial atoms. Only one Si has 3-fold coordination, while the other ones are all 4-fold coordinated. All bonding between a-HfO_2 and a-SiO is formed by Hf-O bonds except one Hf-Si bond.

III. Experimental Measurements.

Deposition and characterization of SiON interfacial layer: SiON interfacial layer was deposited on clean $Si_{0.5}Ge_{0.5}$ (001) substrates by atomic layer deposition (ALD) using 20 cycles of 13.5 MegaLangmuir (ML) of Si_2Cl_6 followed by 20 ML of N_2H_4(g) with substrate temperature of 285°C. Prior to the SiNx ALD, 400 ML of N_2H_4 was dosed at a substrate temperature of 285°C to terminate the surface with NHx groups. In-situ X-ray photoelectron spectroscopy (XPS) was employed to determine the surface composition as a function of processing step (Fig.10). This interfacial layer is Si-rich with 32% more Si than expected for stoichiometric SiON.

MOS capacitors were fabricated after of 40 cycles of HfO_2 ALD ($HfCl_4$ + H_2O) at 300°C on the $Si_{0.5}Ge_{0.5}$ sample passivated by 15 cycles of SiNx ALD. Capacitance-Voltage (C-V) spectroscopy was performed using AC modulation amplitude of 30mV, in the gate bias range of -2 to 2V, at multiple frequencies from 2 KHz to 1 MHz. Fig.11 shows the C-V curves for a $Si_{0.5}Ge_{0.5}$(001) sample cleaned with HF only, in comparison with the sample with SiON interfacial layer. Relative to the device with cyclic HF clean, the addition of an SiON interfacial layer lowered the lower false inversion above 0 eV (Dit bump).caused by large density of interface traps closer to the edge of the conduction band of $Si_{0.5}Ge_{0.5}$(001). This is consistent with sub-stoichiometric SiON improving the interface quality between SiGe and high-k dielectrics.

IV. Conclusion

The comprehensive DFT-MD simulations of interfaces between a-HfO_2 high-K oxide and SiGe substrates with several amorphous interlayers (a-$SiO_{0.8}N_{0.8}$, a-$SiO_{0.4}N_{0.4}$, a-Si_3N_2, a-Si_3N_4 and a-SiO) have been performed. HSE06 hybrid-functional DOS curves and band-decomposed charge densities were calculated. The stack with oxygen deficient a-SiO interlayer demonstrated the superior electric properties. The O- and N-deficient a-$SiO_{0.4}N_{0.4}$ interlayer and the N-deficient a-Si_3N_2 interlayer demonstrated better electrical properties than the respective fully stoichiometric a-$SiO_{0.8}N_{0.8}$ and a-Si_3N_4 interlayer. The sub-stoichiometric layers are superior since they minimize Ge-O and Ge-N bond formation and minimize strain at the interlayer/$Si_{0.5}Ge_{0.5}$(001) interface and consequently disruption of substrate bonds. Experimental studies using an interlayer of SiON formed by N_2H_4(g) + Si_2Cl_6 ALD confirmed that a sub-stiochiometric interface can lower the defect density on $Si_{0.5}Ge_{0.5}$(001).

This work was supported by funding from Applied Materials and Rasirc Corporation.

References

[1] M. Edmonds, T. Kent, E. Chagarov, K. Sardashti, R. Droopad, M. Chang, J. Kachian, J.H. Park, and A. Kummel "Passivation of InGaAs(001)-(2x4) by Self-limiting CVD of a Silicon Hydride Control Layer" J. Am. Chem. Soc., 137 (26), pp 8526–8533 (2015)

[2] K. Sardashti, K.-T. Hu, K. Tung, S. Madisetti, P. McIntyre, S. Oktyabrsky, S. Siddiqui, B. Sahu, N. Yoshida, J. Kachian, B Fruhberger, A. C. Kummel. "Nitride Passivation of the Interface between High-k Dielectrics and SiGe" Appl. Phys. Lett. 108, 011604 (2016).

[3] S. W. Park, H. Kim, E. Chagarov, S. Siddiqui, B. Sahu, N. Yoshida, A. Brandt, and A. C. Kummel " Formation of Chemically Selective Si-O-Al on SiGe(001) and (110) for ALD Nucleation Using HOOH(g); Surf. Sci, 652, p 322-333 (2016)

[4] E. A. Chagarov, L. Porter, A. Kummel, J. Chem. Phys. 144, 084704 (2016).

[5] E. Chagarov, A. Kummel, J. Chem. Phys. 135, 244705 (2011).

[6] E. Chagarov, K. Sardashti, T. Kaufman-Osborn, S. Madisetti, S. Oktyabrsky, B. Sahu, A Kummel, ACS Appl. Mater. & Inter. 7, 26275 (2015).

[7] G. Kresse and J. Hafner, Phys. Rev. B 47, 558 (1993).

[8] G. Kresse and J. Hafner, Phys. Rev. B 49, 14251 (1994).

[9] G. Kresse and J. Furthmüller, Comput. Mat. Sci. 6, 15 (1996).

[10] G. Kresse and J. Furthmüller, Phys. Rev. B 54, 11169 (1996).

[11] P. E. Blochl, Phys. Rev. B 50, 17953 (1994).

[12] G. Kresse and D. Joubert, Phys. Rev. B 59, 1758 (1999).

[13] J. P. Perdew, K. Burke, and M. Ernzerhof, Phys. Rev. Lett. 77, 3865 (1996).

[14] J. P. Perdew, K. Burke, and M. Ernzerhof, Phys. Rev. Lett. 78, 1396 (1997).

[15] J. Heyd, G. E. Scuseria, and M. Ernzerhof, J. Chem. Phys. 118, 8207 (2003).

[16] J. Heyd and G. E. Scuseria, J. Chem. Phys. 121, 1187 (2004).

[17] J. Heyd, G. E. Scuseria, and M. Ernzerhof, J. Chem. Phys. 124, 219906 (2006).

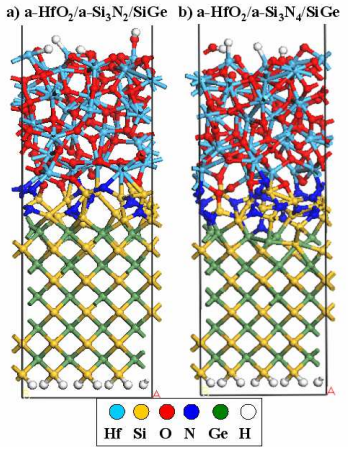

Fig. 1. a) a-HfO_2/a-Si_3N_2/SiGe with a N-deficient interlayer. b) a-HfO_2/a-Si_3N_4/SiGe with a fully-stoichiometric interlayer.

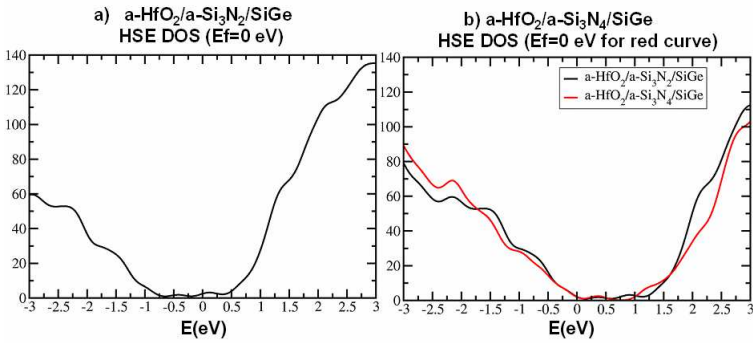

Fig. 2. a) HSE06 DOS for a-HfO_2/a-Si_3N_2/SiGe with N-deficient interlayer. Ef=0 eV. b) HSE DOS for a-HfO_2/a-Si_3N_4/SiGe with a fully-stoichiometric interlayer.Ef=0 eV for the red curve only. The black curve was shifted to align core-level peaks.

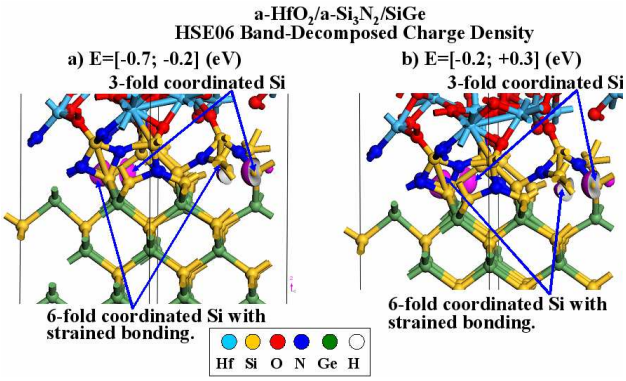

Fig. 3. HSE06 band-decomposed charge density for N-deficient a-HfO_2/a-Si_3N_2/SiGe stack a) the VB state at [-0.7; -0.2] eV is originated by a 3-fold under-coordinated Si and a 6-fold coordinated Si with strained bonding. b) the CB pinning state at [-0.2;+0.3] eV is induced by a 3-fold under-coordinated Si and a 6-fold coordinated Si with strained bonding.

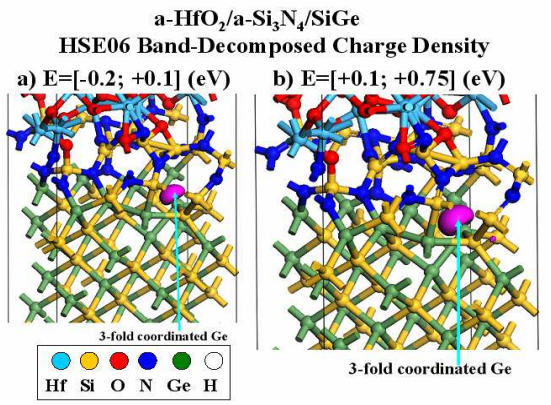

Fig. 4. HSE06 band-decomposed charge density for a-HfO_2/a-Si_3N_4/SiGe stack. a) The state at VB [-0.2; +0.1] eV is induced by a 3-fold under-coordinated Ge. b) The CB pinning state at [+0.1;+0.75] eV is induced by the same 3-fold under-coordinated Ge atom.

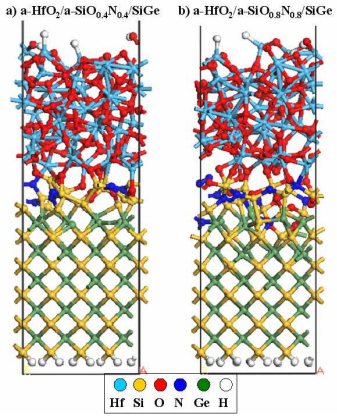

Fig. 5. a) a-HfO_2/a-$SiO_{0.4}N_{0.4}$/SiGe with an O- and N-deficient interlayer. b) a-HfO_2/a-$SiO_{0.8}N_{0.8}$/SiGe with a fully-stoichiometric interlayer.

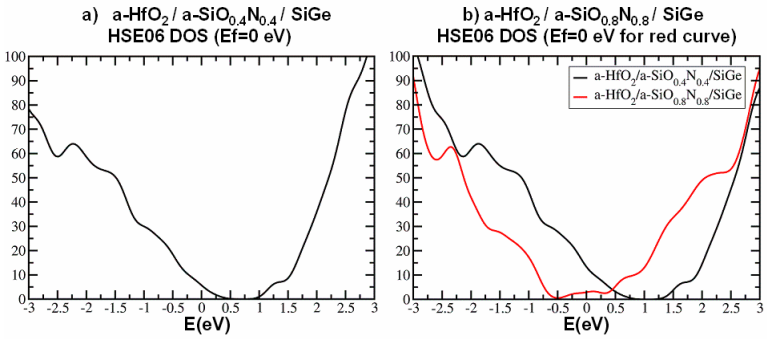

Fig. 6. a) HSE06 DOS for a-HfO_2/a-$SiO_{0.4}N_{0.4}$/SiGe with O- and N-deficient interlayer. Ef=0 eV. b) HSE06 DOS for a-HfO_2/a-$SiO_{0.8}N_{0.8}$/SiGe with a fully-stoichiometric interlayer. Ef=0 eV for the red curve only. The black curve was shifted to align core-level peaks.

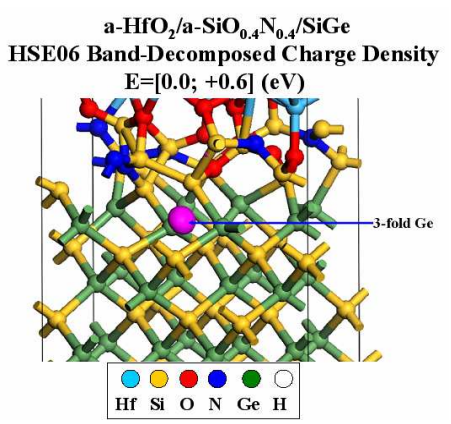

Fig. 7. HSE06 band-decomposed charge density for a-HfO_2/a-$SiO_{0.4}N_{0.4}$/SiGe stack. The VB state at [0.0;+0.6] eV is induced by a 3-fold under-coordinated Ge.

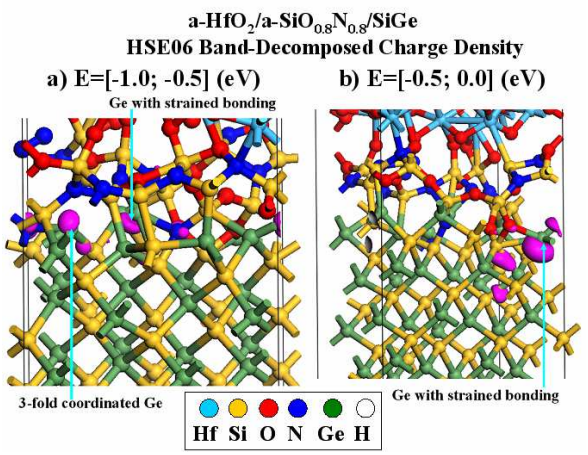

Fig. 8. HSE06 band-decomposed charge density for a-HfO_2/a-$SiO_{0.8}N_{0.8}$/SiGe stack. a) the VB state at [-1.0; -0.5] (eV) is induced by a 3-fold under-coordinated Ge and fully-coordinated Ge with strained bonding. b) the CB state at [-0.5;0.0] (eV) is induced by the same fully-coordinated Ge atom with strained bonding.

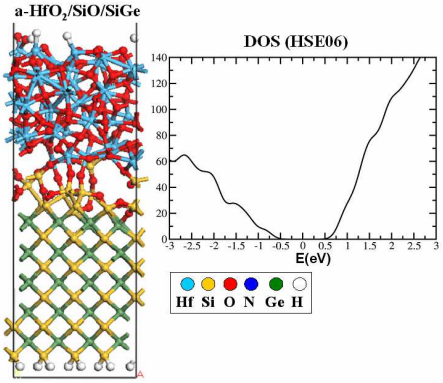

Fig. 9. a-HfO_2/a-SiO/SiGe stack and its HSE06 DOS.

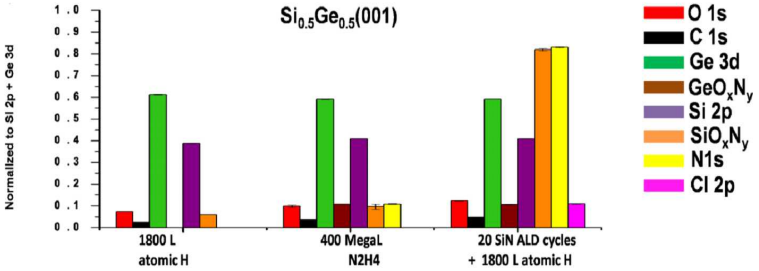

Fig. 10. XPS Derived Surface Compositions of $Si_{0.5}Ge_{0.5}$(110), $Si_{0.5}Ge_{0.5}$(001), $Si_{0.7}Ge_{0.3}$(001) after ALD with N_2H_4(g) and Si_2Cl_6(g) on $Si_{0.5}Ge_{0.5}$(001). XPS corrected peak areas of unshifted Si 2p, unshifted Ge 3d, SiOxNy, GeOxNy, O 1s, C 1s, N 1s, and Cl 2p normalized to the sum of unshifted Si 2p and unshifted Ge 3d peaks following an 1800 Langmuir atomic hydrogen dose at 330°C, 400 MegaLangmuir N_2H_4 dose at 285°C, and following an additional 20 SiNx ALD cycles and final atomic hydrogen dose at 285°C.

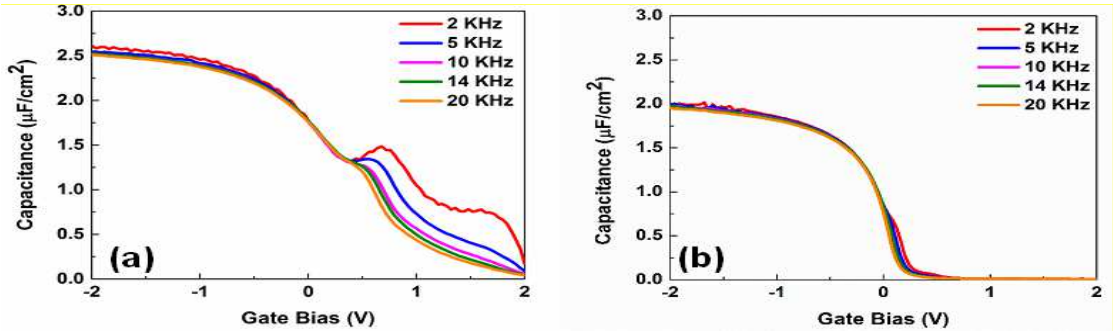

Fig. 11. C-V characteristics of $Si_{0.5}Ge_{0.5}$(001) MOSCAPs with 40 cycles of HfO_2 deposited by ALD. C-V spectra of (a) HF cyclic clean and (b) 15 cycles of SiNX ALD. Due to low substrate doping and large series resistance, only the low-frequency C-V characteristics at 2 – 20 kHz are shown here. SiON interfacial layer reduced the size of the false inversion capacitance (Dit bump) due to interfacial defects for Vg > 0V.